A Nonlinear Switch Based on Irregular Structures and Nonuniformity in Doped Photonic Crystal Fibers

Fathi AbdelMalek, Hongbo Li, Axel Schülzgen, Jerome V. Moloney, Nasser Peyghambarian, *Member, IEEE*, Huseyin Ademgil, and Shyqyri Haxha, *Senior Member, IEEE*

***Abstract*—We propose a novel nonlinear switchbased on the irregularity in a three-core-doped photonic crystal fiber (PCF). We numerically investigate the proposed structure, which consists of air holes arranged in a triangular lattice around two defects separated by a single Er-Yb doped core. Its switching operation is based on the gain change in the doped core due to the nonuniformity and irregular structure around it. It is shown that by adjusting the gain in the doped core, the light is entirely transferred from the central core to the upper and lower ones. We have employed the full vectorial finite-element method and the finite-difference time domain to investigate and optimize the optical modes, nonlinear parameter, and gain effects on the switching operation. It is found that an optimum gain is essential to allow either a periodic exchange of the light between the upper and lower cores or independent core propagation. Possible nonuniformity in the hole diameters and irregularity problems of the proposed PCF design during the fabrication process have been predicted. The waveguide dispersion with respect to the doped central core region has been thoroughly investigated.**

***Index Terms*—Birefringence, chromatic dispersion, optical switches, photonic crystal fibers.**

I. Introduction

PHOTONIC CRYSTAL fibers (PCFs) are receiving growing attention in the photonics community [1]–[3] due to their unique propagation characteristics and dispersion properties. These microstructures offer new possibilities for nonlinear applications as they possess a very small mode area that enhances the nonlinearity. Due to these characteristics, compact nonlinear devices can be realized, offering tremendous benefits in all-optical signal processing on a single platform.

Manuscript received April 23, 2008; revised September 18, 2008. Current version published May 13, 2009.

F. AbdelMalek is with the College of Optical Sciences, University of Arizona, Tucson, AZ 85721-0094 USA, and also with the National Institute of Applied Sciences and Technology (INSAT), BP 676 1080 Tunis Cedex, Tunisia (e-mail: fathi_abdelmalek@yahoo.com).

H. Li is with the College of Optical Sciences, University of Arizona, Tucson, AZ 85721-0094 USA, and also withAither Engineering, Lanham, MD 20706 USA (e-mail: hongbo@e-mail.arizona.edu).

A. Schülzgen and N. Peyghambarian are with the College of Optical Sciences, University of Arizona, Tucson, AZ 85721-0094 USA (e-mail: axel@u.arizona.edu; nnp@u.arizona.edu).

J. V. Moloney is with the College of Optical Sciences, University of Arizona, Tucson, AZ 85721-0094 USA, and also with the University College Cork, Cork, Ireland (e-mail: jml@acms.arizona.edu).

H. Ademgil and S. Haxha are with the Photonics Group, Department of Electronics, University of Kent, Canterbury CT2 7NT, U.K. (e-mail: ha62@kent.ac.uk; s.haxha@kent.ac.uk).

Color versions of one or more of the figures in this paper are available online at http://ieeexplore.ieee.org.

Digital Object Identifier 10.1109/JQE.2009.2013144

The guiding of light in PCFs can be realized via one of the two mechanisms: effective index guidance and photonic bandgap (PBG) guidance. For effective-index-based PCFs, the effective refractive index of the composite material (or cladding) is lower than the refractive index of the higher index core, which makes it possible to trap the light in the core region made of the higher index material. The light is therefore confined by total internal reflection (TIR) [4]. On the other hand, PCFs based on the PBG have the capability to guide the light within a certain frequency band [5]–[7]. PCFs have many remarkable properties, strongly dependent on the design details such as low sensitivity to bend losses even for large mode areas, small or large mode areas leading to very strong or weak optical nonlinearities. This property may be achieved with a lower numerical aperture than a conventional fiber [8].

In the last decade, Er-doped fiber lasers have been thoroughly investigated [9]. Er-doped fibers are widely used in the form of trivalent ion Er as the laser-active dopant of gain media based on various host materials. It exhibits a high threshold pump power. Many energy transfer processes can occur, particularly for high doping concentrations [10].The main applications are in Er-doped fiber amplifiers for switching applications in optical fiber communication systems [11]. Nonlinear Er-doped fibers can offer many options for realizing couplers, solitons, and switches [12]. The pioneering work of Janos and Minasian [13] demonstrated that optical switches suffer from high pump power and very long switching time. This is a result of the refractive index variations due to the low gain, which is mainly due to the lifetime of the metastable state, which is about 10 ms [14]. Chen *et al.* [15] studied a twin-core coupler that includes both gain and losses. They have demonstrated that the gain plays an important role in reducing the switching power as well as reducing the device length. On the other hand, the introduction of loss in the other core has a strong effect in the switching process. Twin-core Er-doped fibers have been used to realize a nonlinear switch [16], which is a key component for the design and fabrication of all-optical fiber switches. In all-optical switches using silicon photonic crystal nanocavities, the operating power can be reduced significantly [17] due to the fact that in a small volume of the nanocavities, the photon density becomes very high, and subsequently, a large power reduction can be achieved. Recently, it was demonstrated that Er-doped fiber-based lasers offer excellent stability that can be used in potential applications such as wavelength-division multiplexing (WDM) systems [18], [19]. Liu *et al.* [20]has proposed a new type of Er-doped PCF lasers with high performances in terms of self-stability and uniformity due to the high

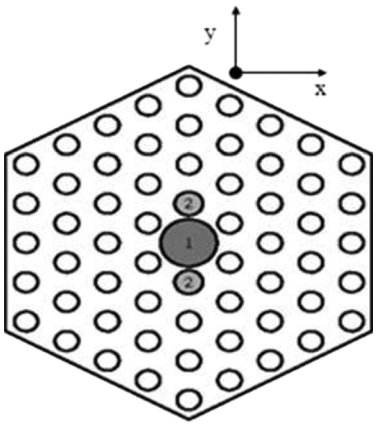

Fig. 1. Doped three-core PCF structure.

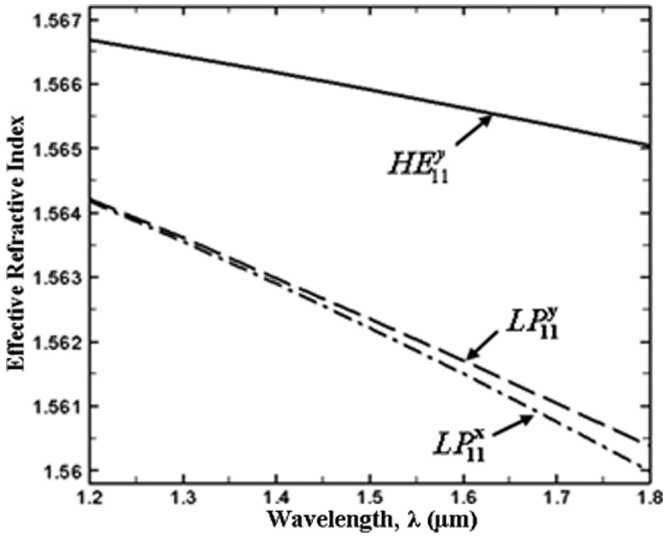

Fig. 2. Variation of the effective refractive index of the fundamental and higher order modes as a function of the operating wavelength.

nonlinearity in the doped core of the PCF. The PCF nonlinearity can be affected by altering the shape, size, and position of the air holes. Changing the mode size alters the nonlinearity of the fiber by increasing or decreasing the power inside the fiber. This either increases or decreases the nonlinear phase change that is experienced by the light during propagation [21].

Additionally, proper design of the dispersion allows PCFs to generate nonlinear frequency by using the strong nonlinearity property. Recently published papers have shown that multiple-core PCFs offer many new applications such as couplers, splitters [22]–[25], and switches [3]. Mangan *et al.* [26] demonstrated that twin-core PCFs-based couplers have a wide coupling length range by optimizing the design parameters such as the hole size and the hole-to-hole spacing [26].

In this paper, we propose a novel nonlinear three-core PCF switch. The switching operation and key fabrication parameters of the proposed design are investigated. The central core is doped with Er-Yb ions, whereas the upper and lower cores are undoped. Light coupling between the upper and lower cores is achieved by change in gain. The nonuniformity in hole diameters and irregularity issues that can be introduced during the fabrication process have been thoroughly investigated. Additionally, nonlinearities, effective mode area, and waveguide dispersion properties of the proposed design have been studied.

II. Simulation Results

The PCF considered in this study is composed of air holes arranged in a triangular lattice centered around three-core defects, as shown in Fig. 1. The central core is doped with Er-Yb ions, while the upper and lower cores are undoped. The PCF considered in this study is assumed to be made of phosphate glass, which has a higher refractive index (around 1.56) than that of fused silica. It is well known that much higher doping levels of Er and Yb ions can be achieved without the detrimental clustering effect in phosphate glass than in silica glass. As a result, high gain coefficient, necessary for the nonlinear optical switch, can be obtained in a PCF made of phosphate glass. The PCF structure is described by the air hole diameter (d) and the air hole separation or pitch (Λ). The doped core marked as 1 (Core1) has a diameter of 1.2Λ and a complex refractive index [27]

$$\Delta\tilde{n} = \Delta n + j(\lambda/2\pi)\Delta\alpha \tag{1}$$

where $\Delta n = 1.5683$ is the real part of $\Delta\tilde{n}$, and $\Delta\alpha$ represents either a gain or loss. Upper and lower cores of which are marked as 2 (Core2) have a diameter of 0.6Λ, and a refractive index equal to 1.5664. Air holes in the cladding region have a diameter of 0.5Λ. In designing PCFs, either the gain or the loss is a fundamental parameter and is related to the imaginary part of the complex propagation constant, which is directly dependent on the imaginary part of the complex refractive index.

Initially, in order to show that the proposed PCF switch supports both the fundamental and second-order hybrid modes, we investigated the effective refractive index of the fundamental and higher order modes. Fig. 2 illustrates variation of the effective refractive index as a function of the operating wavelength when the following core dimensions are considered: Core1 $=$ 11.4 μm and Core2 $=$ 5.7 μm. The LP_{01} (HE_{11}) fundamental mode is represented by the solid curve, whereas the dashed curve represents the second-order $LP11$ modes along the y-direction, and dashed-dotted curve represents the LP_{11} mode along the x-direction [28]. The upper and lower cores have a higher refractive index than the background. As a result of this, the LP_{11}^{y} mode has a slightly higher effective refractive index than the LP_{11}^{x} mode. In our proposed design, Core1 and Core2 have a higher refractive index than the background; $|n_{\mathrm{Core1}} - n_{\mathrm{Core2}}| = 1.9 \times 10^{-3}$, $|n_{\mathrm{background}} - n_{\mathrm{Core2}}| = 1.97 \times 10^{-2}$, and $|n_{\mathrm{background}} - n_{\mathrm{Core1}}| = 2.16 \times 10^{-2}$. The index difference between Core2 and the background material makes the LP_{11}^{y} mode have an effective refractive index slightly higher than the LP_{11}^{x} mode. Due to the fact that the materials that are used in both upper and lower cores have higher effective index than background, the LP_{11}^{y} mode leaks/couples through to

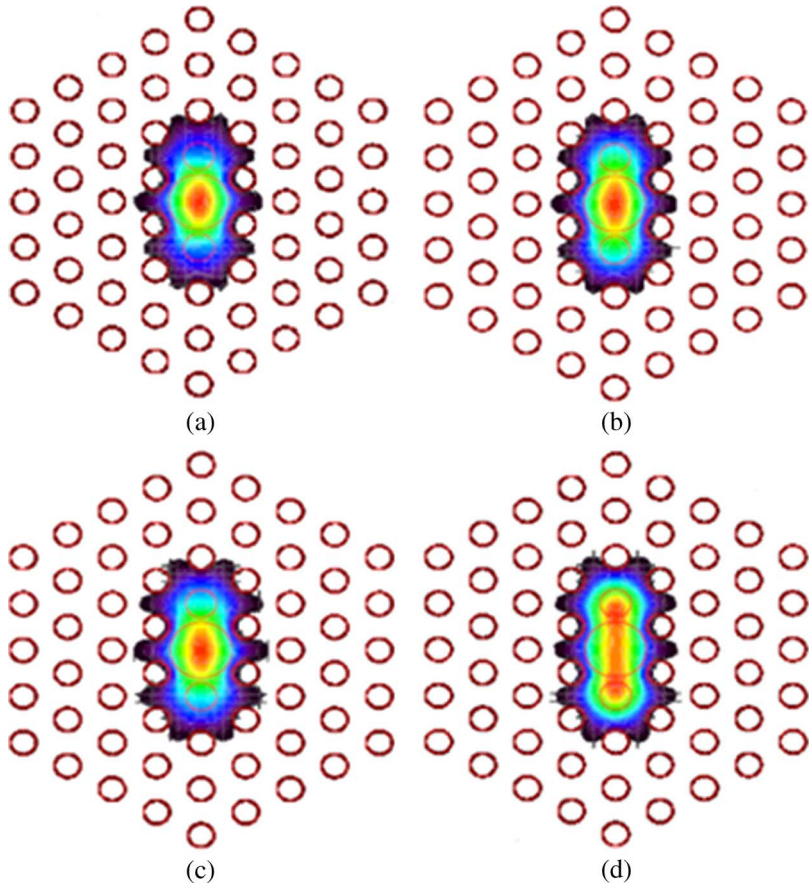

Fig. 3. (a) E_x component of the fundamental HE_{11}^y mode, when $\Delta\alpha = 0$ cm^{-1}. (b) E_y mode of the electric field, when $\Delta\alpha = 0$ cm^{-1}. (c) E_x mode of the electric field, when $\Delta\alpha = 0.7$ cm^{-1}. (d) E_y mode of the electric field, when $\Delta\alpha = 0.7$ cm^{-1}.

both the upper and lower cores readily. The fundamental mode is much better confined than the higher order modes, and as a result of this, its effective refractive index is closer to the core index. The difference between the effective refractive indexes of the two fundamental polarization modes (HE_{11}^x and HE_{11}^y) is very small, around 10^{-5}. Therefore, throughout the paper, we investigate only the HE_{11}^y (shown by the solid curve) modal properties of the proposed PCF switch.

In this study, we assume that the doped core has both a real refractive index step Δn and a gain coefficient $\Delta\alpha$. The complex refractive index step is given by (1), considering only the gain effect, which means that $\Delta\alpha$ is positive. The imaginary part of the refractive index is about 0.2410^{-4} [27]. The changes in pump light intensity modify the gain, which in return perturbs the refractive index of the central core. The existence of gain in central core is found to be responsible for the decrease in switching power and shortening the device length while the introduction of the loss in the upper and lower cores plays a role of idealizing switching [15]. The light switching is based on the nonlinear refractive index modulation. The Er concentration in a phosphate fiber can be as high as a few percent and the Yb concentration can be over 10%. For such high doping concentration, moderate pump power can generate the required gain for the optical switching, depending on the signal power level and the pump scheme. Since the gain is dependent on the signal power level, the gain is the most important factor for this nonlinear switching.

In order to analyze the switching operation, full vector finite-element method (FEM) is used to find the propagating modes [29], [30]. The FEM is a powerful numerical tool able to deal with many complex structures and provide full vector analysis of different photonic waveguide devices, including PCFs [29]–[31]. In the FEM formulation, the domain is divided into many subdomains with triangular-shaped elements in such a way that the step index profiles can be exactly represented. The light propagation and power distribution are carried out by employing the finite-difference time domain (FDTD) method [32]–[34]. Initially, $\Delta\alpha$ is set equal to 0, then the electric field of the fundamental mode for both polarizations is calculated and illustrated in Fig. 3(a) and (b). As may be seen from Fig. 3(a), the E_x component of the HE_{11}^y mode is more confined in the central core than its counterpart E_y component. This confinement feature of the mode to the core region is linked to how much the mode expands toward the adjacent cores. The confinement factor of a given mode is defined as the ratio of the modal power propagating in the fiber core to the total power of the mode. The effective refractive index of a mode, as a result, is related to its confinement factor. A higher effective refractive index indicates a better modal confinement. It is worth noticing that E_x component is slightly modified compared to the E_y

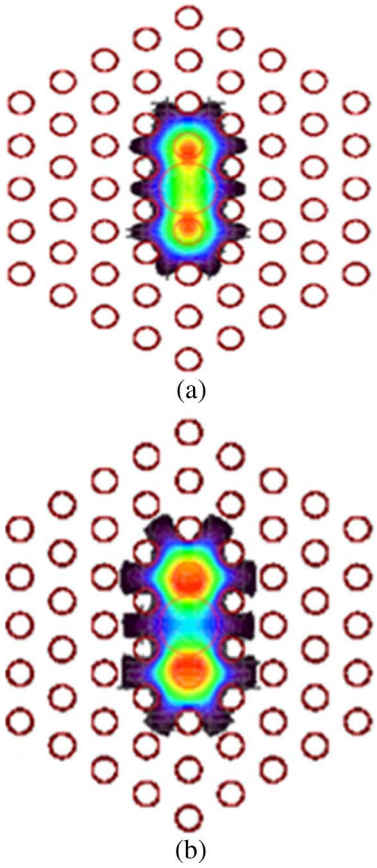

Fig. 4. Modal field expansion, E_y component of the fundamental HE_{11}^y mode. (a) $\Delta\alpha = 0.8$ cm^{-1}. (b) $\Delta\alpha = 0.85$ cm^{-1}.

component, while the light remains confined in the central core and is not coupled to the upper and lower cores. In order to study the gain effect on the modal field expansion and the coupling between cores, $\Delta\alpha$ is varied. Our simulations show that when $\Delta\alpha$ ranges from 0.1 cm^{-1} to 0.7 cm^{-1}, the E_x and E_y components of HE_{11}^y mode are still confined in the central core. Results of E_x and E_y when $\Delta\alpha = 0.7$ cm^{-1} are illustrated in Fig. 3(c) and (d), respectively. When $\Delta\alpha$ increases from 0.7 cm^{-1} to 0.8 cm^{-1}, we note that there is a power outflow from the doped core to the upper and lower ones, which is induced by axial gain, as shown in Fig. 4(a). Also, Fig. 4(a) shows that the E_y component of fundamental HE_{11}^y mode expands toward the upper and lower cores, and consequently, the coupling operation is expected to take place. We can draw the conclusion that the key parameter of the switching operation is the critical value of the gain. The coupling and switching operations are strongly depending on the minimum required gain. The gain parameters depend on factors such as the waveguide structure and the external pump. As a result, the external pump can be properly adjusted to compensate the effect of the waveguide structure so that the nonlinear switch can be achieved. This is an important characteristic of three-core PCF structures with a single doped core.

Next, our study focuses on the switching operation, as we increase $\Delta\alpha$ to 0.85 cm^{-1}. Fig. 4(b) shows the modal field expansion of E_y component, where $\Delta\alpha = 0.85$ cm^{-1}. The mode in the central core is transferred to the upper and lower cores. Furthermore, the entire field in the central core is completely transferred to the upper and lower ones, when $\Delta\alpha = 0.85$ cm^{-1}, as shown in Fig. 4(b). This is due to the nonlinear refractive index modulation that causes resonance frequency that shifts when the pump power increases. Also, due to the fact that structures with larger hole sizes demand a smaller air hole separation, a smaller mode area can be achieved. The small mode area increases the nonlinearity, and therefore, both the power and time switching can be reduced. Chu and Wu [35] have demonstrated that by increasing the input power from 13 μW to 0.93 mW, the light switches from one core to another. Also, this switching operation is maintained until the input power reaches 5 mW, which constitutes the saturation level [35]. To explain whether this process is due to either nonlinear or thermal effects, an experimental work was carried out by Betts *et al.* [36]. In their work [36], they launched two light beams at different wavelengths along a dual-core fiber. They found that the green light shifts, while the red light did not shift. From this achievement, one may conclude that the process is due to nonlinear effect and dispersion. The pulse switching is related to the dispersion length and can be written as [3]

$$L_D = \tau^2 2\pi c/\lambda^2 D \tag{2}$$

where τ represents the pulsewidth, D is the dispersion, and c is the speed of light in vacuum. At shorter wavelengths, with a small pulsewidth, the dispersion length is high and the switching operation can take place. However, at larger wavelength, L_D decreases and can be ignored. When the pulsewidth is large and the dispersion D is small, L_D becomes large and light can be switched. However, when the pulsewidth is small, the pulse remains in the core confined and its switching depends strongly on the parameter D. In the Er-doped PCF, the pulsewidth is small, which may result in a slow switching operation and an increase of the loss. The confinement loss of the PCF can be reduced significantly by increasing the number of air holes. PCF with larger hole sizes results in a greater core isolation, and therefore, smaller effective mode area, and in return, the nonlinearity would be increased. As a result of these effects, the switching operation is easier to be achieved. The main effect of the wavelength is the maximum gain that can be achieved in the core. The maximum gain/loss occurs at the resonance wavelength of the Er ion, close to 1.55 um.

In this paper, we have also investigated the birefringence properties of the proposed PCF design. Birefringence is defined as the difference between the effective refractive indexes of two fundamental polarization modes (HE_{11}^x and HE_{11}^y) and can be written as [37]

$$B = |n_x - n_y| \tag{3}$$

where n_x and n_y are the effective refractive indexes of each fundamental mode. The birefringence in PCFs can reduce the coupling between the orthogonal states of the fundamental mode. It is also worth mentioning that in many sensing applications and applications where light is required to maintain a linear

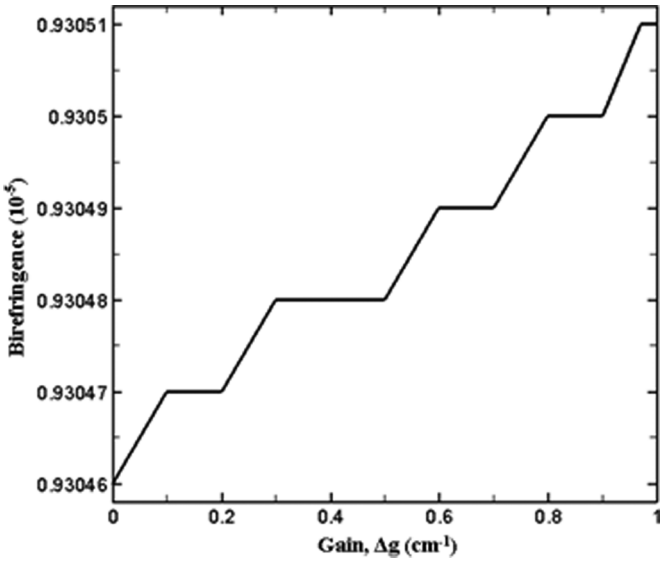

Fig. 5. Variation of birefringence as a function of the gain.

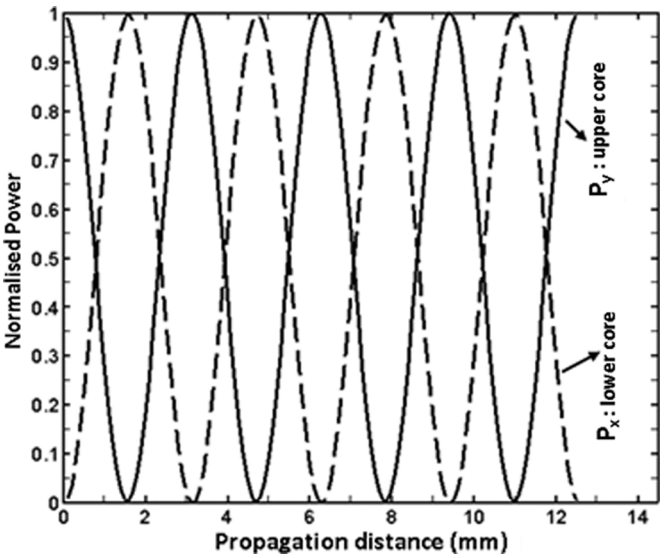

Fig. 6. Normalized power with the propagation distance when the upper and lower cores are coupled.

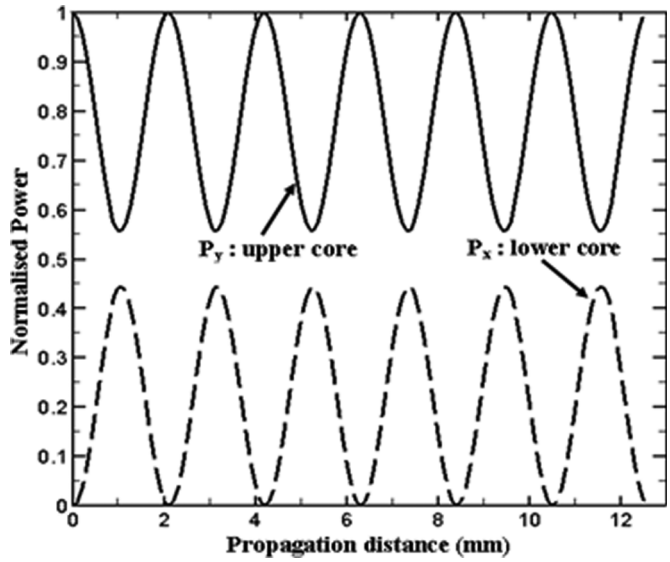

Fig. 7. Normalized power propagation while both cores are not coupled.

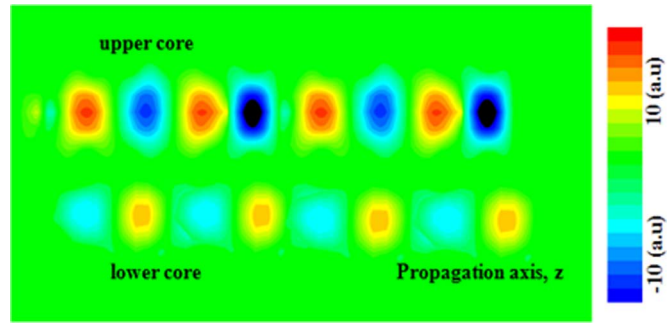

Fig. 8 Field pattern in the uncoupled cores.

polarization state, a high level of birefringence is often necessary [38]. The introduced imperfections during fabrication process can create asymmetries that break the degeneracy and bring out unintentional birefringence [39]. The later increases with the difference in refractive index of x and y polarized modes. Therefore, we have investigated the effects of $\Delta\alpha$ on the birefringence, and the results are illustrated in Fig. 5. Here, the birefringence is defined as the difference in the index of the x and y polarized modes. It can be clearly seen that when Δn increases, $\Delta\alpha$ also increases. Minimum birefringence is achieved when $\Delta\alpha = 0$. This clearly indicates that the introduced defects generate the birefringence; PCF with larger air holes experience a greater birefringence than PCFs with smaller air holes [29], [40].

The power in the upper and lower cores as a function of the propagation distance is shown in Fig. 6. Since the lower and upper cores are identical, the power is distributed equally between them. Power oscillations between these two cores are mainly due to the mode beating phenomenon. One can see that when the mode propagates along the PCF, the power is completely transferred from one core to the other at a propagation distance of about 1.7 mm.

Fig. 7 shows the variation of the normalized power as a function of the propagation distance when the upper and lower cores are not coupled. In this case, $\Lambda = 9.5\ \mu$m and the diameter of the upper core slightly changes in comparison to the lower core. It can be observed that the power in the upper and lower cores is not distributed equally. To further underpin this observation, we investigate the field propagation in both the upper and lower cores by employing the FDTD method, and these results are shown in Fig. 8. It can be observed from this figure that the fields are confined in both cores with different amplitudes. It is relevant to note that by optimizing the gain and using different types of defects-based cores, the light can be totally transferred from the doped core to the upper and lower cores.

From the manufacturing viewpoint, the proposed PCFs design can be easily fabricated with the current progress in PCF technology, which has demonstrated that fabrication of even more complex PCF structures is possible. Unfortunately, possible errors or various imperfect fabrication conditions, as in any

PCF structure, could affect the light propagation characteristics of the proposed design. Therefore, fabrication error possibilities, such as the variation of hole size and hole-to-hole spacing, have been investigated. The fabrication tolerances have been previously discussed by Poletti *et al.* [41]. In this paper [41], dispersion of the proposed PCF design is investigated by changing the air hole sizes and the hole-to-hole spacing by $\pm 1\%$, $\pm 2\%$, $\pm 5\%$, and $\pm 10\%$ from the optimum value. One can see from this paper that nonuniformities affect the propagation and this results in variations in dispersion values. In addition, Reichenbach and Xu [40] have shown that nonuniformities occurring in cladding area are affecting the birefringence and zero-dispersion wavelength. Tolerances from the literature on PCF manufacturing are between $\pm 1\%$ and $\pm 10\%$. Therefore, we have decided to take it as $\pm 5\%$.

Awareness of the sensitivity of different fiber properties having hole-to-hole spacing deficiency and the degree of structural variations that can be tolerated will also be helpful tools for future PCF designs. Such investigation can be carried out through calculations of effective mode area A_{eff}, which is one of the key parameters in designing PCFs. The effective area of the core area can be calculated using [8]

$$A_{\text{eff}} = \frac{\left(\int\int |E^2| dxdy\right)^2}{\int\int |E|^4 dxdy}. \tag{4}$$

It is known that a low effective area provides a high density of power needed for nonlinear effects to be significant. However, the effective area can also be related to the spot size, with the Gaussian width w, through $A_{\text{eff}} = \pi w^2$, and thus, it is also important in the context of confinement loss, microbending loss, macrobending loss, splicing loss, and numerical aperture [42]. Here, in this study, we investigated the effective mode area of the proposed PCF structure as a function of the operating wavelength.

Variation of the effective area as a function of the operating wavelength where diameter of Core1 and Core2 has changed to $\pm 5\%$ is presented in Fig. 9. The dashed line represents the case where $\text{Core1} = 11.4\ \mu\text{m}$, $\text{Core2} = 5.7\ \mu\text{m}$, and the effective area is 62.3 μm^2 at a wavelength of 1.55 μm. As can be seen from this figure, the effective area of the coupled fundamental HE_{11}^{y} mode increases when diameter of the central core (Core1) increases $+5\%$ and drastically decreases when the diameter of the central core decreases. At the shorter wavelengths, the effective area of coupled mode increases significantly when the upper and lower core sizes decrease. On the other hand, one can see that at longer wavelengths, the effective area has slightly changed when the diameter of the upper and lower cores has changed to $\pm 5\%$. It is apparent that, at longer wavelengths (between 1.4 and 1.8 μm), variation of the central core size does not significantly affect the effective mode area.

The dispersion caused by the wavelength dependence of the nonlinearity counteracts the dispersion of the fiber, and thus, the pulses do not become wider as much as it is expected by taking into account constant parameter values for dispersion and

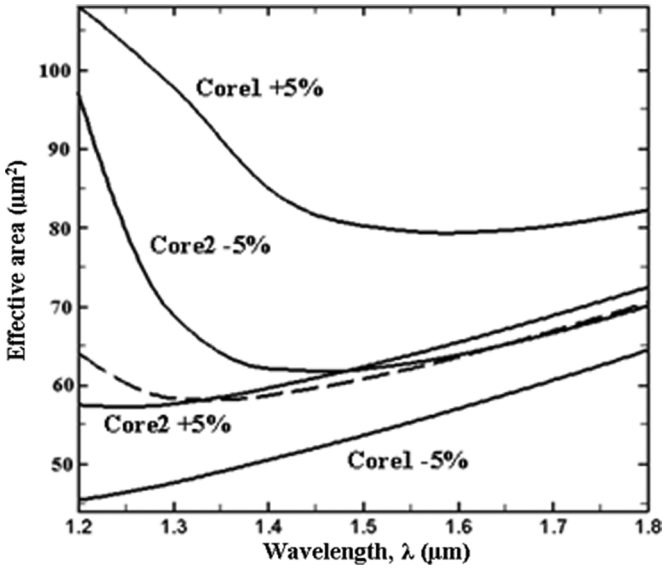

Fig. 9. Variation of effective area as a function of the wavelength where nonuniformity of holes diameter investigated, when $\Lambda = 9.5\ \mu$m and $\Delta g = 0.8\ \text{cm}^{-1}$. Dashed line represents the case where $\text{Core1} = 11.4\ \mu$m and $\text{Core2} = 5.7\ \mu$m.

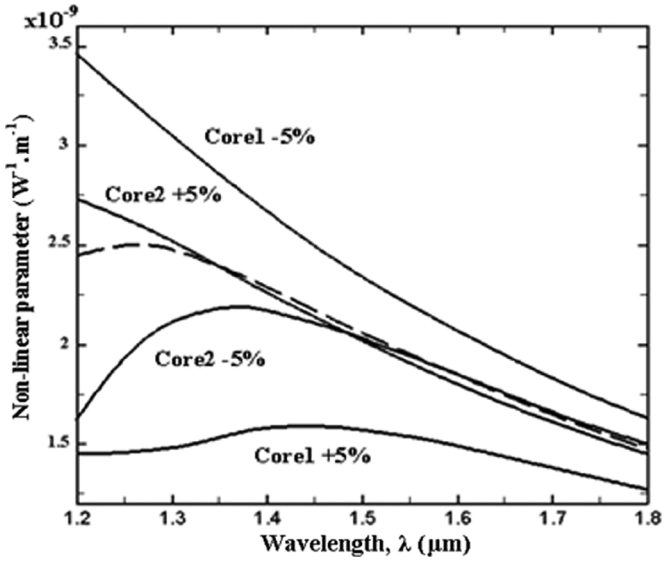

Fig. 10. Variation of nonlinear parameter γ as a function of the wavelength when $\Lambda = 9.5\ \mu$m and $\Delta\alpha = 0.8\ \text{cm}^{-1}$ where diameter of Core1 and Core2 has been increased and decreased by 5%. Dashed line represents the case where $\text{Core1} = 11.4\ \mu$m and $\text{Core2} = 5.7\ \mu$m.

nonlinearity. The nonlinear parameter is inversely proportional to the effective area and can be calculated from [43]

$$\gamma(\lambda) = \frac{2\pi}{\lambda} \frac{n_2}{A_{\text{eff}}(\lambda)} \tag{5}$$

where $n_2 = 3 \times 10^{-20}\ \text{m}^2/\text{W}$ is the nonlinear index coefficient [43]. PCF design presented in [3] has material with nonlinear refractive index 400 times that of silica. Therefore, nonlinearities are expected to be much higher than our proposed design.

Fig. 10 illustrates the variation of the nonlinear parameter as a function of the operating wavelength. Dashed line represents the case when $\text{Core1} = 11.4\ \mu$m, $\text{Core2} = 5.7\ \mu$m,

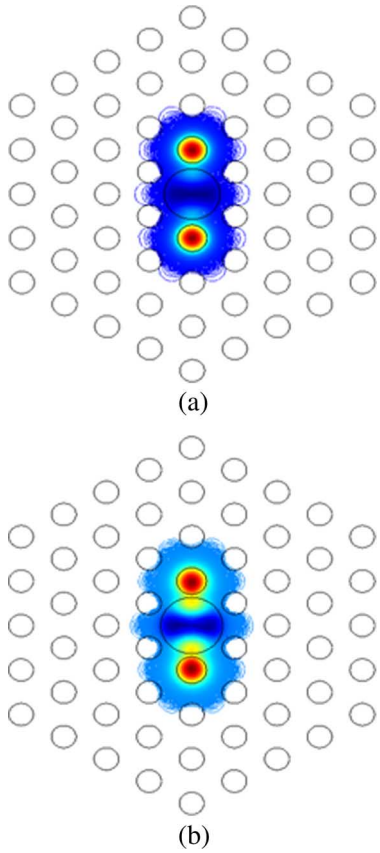

Fig. 11. Field profile of the dominant E_y component of the fundamental HE_{11}^y mode, when core diameters have been changed to $\pm 5\%$ at wavelength $\lambda = 1.55\ \mu$m. (a) Core1 -5%. (b) Core1 $+5\%$.

and $\gamma = 1.95 \times 10^{-9}\ \mathrm{W}^{-1} \cdot \mathrm{m}^{-1}$ at the operating wavelength $1.55\ \mu$m. As can be seen from this figure, the nonlinear parameter for all cases decreases when the wavelength increases, except when the diameter of the Core1 increases for 5%. In this case, the nonlinear parameter is almost flattened. The nonlinear parameter is more affected by the nonuniformity of central core, since it is directly related to the effective area.

The field profiles of the dominant E_y component of the fundamental HE_{11}^y coupled mode is shown in Fig. 11 when the nonuniformity of hole diameters ($\pm 5\%$) is investigated at $\lambda = 1.55\ \mu$m. Fig. 11(a) and (b) illustrates the case when Core1 is distorted for -5% and $+5\%$, respectively, while Core2 is kept fixed. As may be observed from Fig. 11(a), the mode couples easier when the central core diameter decreases by 5%. However, when the size of the Core1 increases by 5%, it can be clearly seen from Fig. 11(b) that mode leaks to the central core. In other words, the mode [in Fig. 11(b)] has not been transferred completely to the upper and lower cores. At the operating wavelength of $1.55\ \mu$m, the nonlinear parameters of the proposed design for -5% and $+5\%$ are reported as $2.2 \times 10^{-9}\ \mathrm{W}^{-1} \cdot \mathrm{m}$ and $1.53 \times 10^{-9}\ \mathrm{W}^{-1} \cdot \mathrm{m}$, respectively, where it is $1.95 \times 10^{-9}\ \mathrm{W}^{-1} \cdot \mathrm{m}$ at ideal position.

In order to investigate the effects of the central core on the robustness and sensitivity of the proposed PCF structure, rms_γ is calculated. The rms is generally used to describe the average

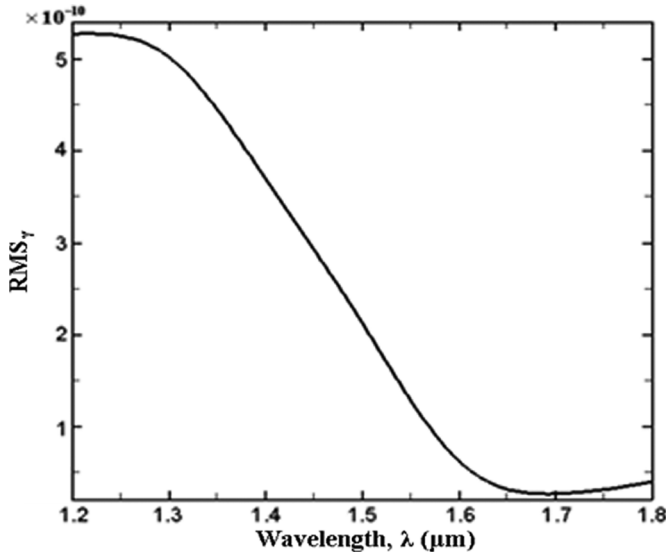

Fig. 12. Variation of rms_γ as a function of the wavelength when $\Lambda = 9.5\ \mu$m and $\Delta\alpha = 0.8\ \mathrm{cm}^{-1}$ where diameter of $\mathrm{Core1} = 11.4\ \mu$m and $\mathrm{Core2} = 5.7\ \mu$m (ten different positions have been considered: $x = 0$ and $y = 0$, $x = 0.2\ \mu\mathrm{m} - 0.6\ \mu\mathrm{m}$ and $y = 0$, $x = 0$ and $y = 0.2\mu\mathrm{m} - 0.6\ \mu$m, $x = 0.2\ \mu\mathrm{m} - 0.6\ \mu$m and $y = 0.2\ \mu\mathrm{m} - 0.6\ \mu$m).

effect related to the nonlinearity coefficient in analyzing random processes, and can be defined as

$$\mathrm{rms}_\gamma = \sum_{i=1}^{N} \sqrt{\frac{(\gamma_i - \bar{\gamma})^2}{N(N-1)}} \tag{6}$$

where N is the total number of samples, i is the consideration of random distributions of the cores when the irregularity is investigated, and $\bar{\gamma}$ is the average value of the nonlinear coefficient.

The maximum of rms is reached at $\lambda = 1.2\ \mu$m, where the disorder of cores makes it more dispersive. The core disorder allows γ to deviate from the ideal value; similarly, the chromatic dispersion fluctuates and shifts from its ideal value. At the optimum position, the standard deviation of rms is about 0.19×10^{-10}, the perturbation accounts for all errors.

Fig. 12 shows the variation of rms_γ as a function of the wavelength when $\Lambda = 9.5\ \mu$m, $\Delta\alpha = 0.8\ \mathrm{cm}^{-1}$, Core1 diameter is $11.4\ \mu$m, and Core2 diameter is $5.7\ \mu$m. In these simulations, ten different positions of central core have been considered. Owing to the symmetry of the structure, position of the central core is moved only in $+x$ and $+y$ directions. The following positions are considered: ($x = 0$ and $y = 0$), ($x = 0.2\ \mu\mathrm{m} - 0.6\ \mu$m and $y = 0$), ($x = 0$ and $y = 0.2\ \mu$m: $0.6\ \mu$m), and ($x = 0.2\ \mu$m: $0.6\ \mu$m and $y = 0.2\ \mu$m: $0.6\ \mu$m). One can see that the rms_γ effect that is related to the nonlinearity coefficient decreases as the wavelength increases from 1.2 to 1.65 μm, then it gradually starts to increase as the wavelength increases from 1.65 to 1.8 μm.

A study of dispersion in PCFs is essential for practical applications in optical communication systems, dispersion compensation, and linear/nonlinear optics. Chromatic dispersion [44]–[47] is the main factor contributing in optical pulse broadening. Therefore, it is vital to calculate the chromatic

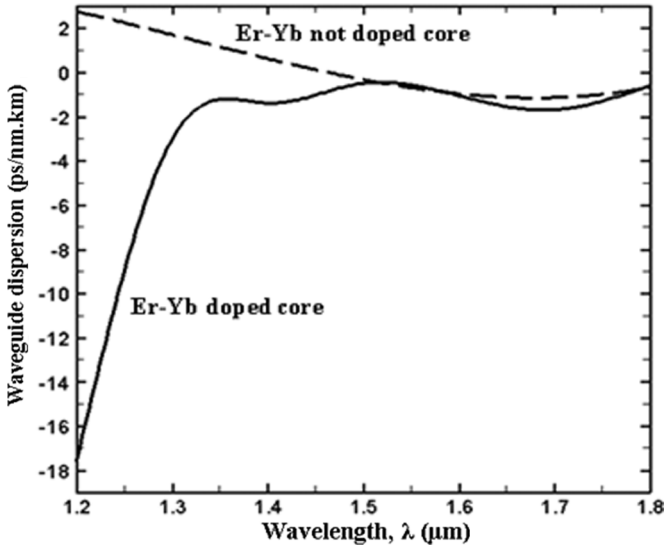

Fig. 13. Variation of the waveguide dispersion of coupled HE_{11}^{y} mode as a function of the wavelength where doped and undoped central cores are used.

dispersion, which is caused by the combined effects of material and waveguide dispersions

$$D = -\frac{\lambda}{c}\frac{\partial^2 \mathrm{Re}(n_{\mathrm{eff}})}{\partial \lambda^2} \tag{7}$$

where c is the velocity of light and $\mathrm{Re}(n_{\mathrm{eff}})$ is the real part of n_{eff}. Material dispersion refers to the wavelength dependence of the refractive index of the material caused by the interaction between the optical mode and ions, molecules, or electrons in the material. Waveguide dispersion depends on the core diameter and the refractive index contrast between the core and the cladding. In this study, the material dispersion is not considered since three different materials with different refractive indexes have been used, and each material has unique dispersion properties; for this reason, it is not possible to simulate exact calculation of chromatic dispersion.

Fig. 13 shows variation of the waveguide dispersion of coupled HE_{11}^{y} mode as a function of the wavelength when doped and undoped central cores are used. One can see that the proposed PCF exhibits a high performance in terms of waveguide dispersion. Nearly zero and ultraflattened dispersion across a wide wavelength $(1.4$–$1.8\ \mu\mathrm{m})$ is obtained for both cases. At shorter wavelengths, the dispersion difference between PCFs with doped and undoped central core is higher than at longer operating wavelengths. Since the mode couples more in the upper and lower core levels, doping of the central core does not affect much the dispersion at longer wavelengths. It is known that nearly zero and flattened dispersion across a wide wavelength would have tremendous potential for future applications such as high bit rate communication systems, polarization maintaining devices, and sensing systems. Integrated optical sensors with arms require an optical switch with a relatively slow switching time. Typically, these optical sensors consist of two arms, where the first arm can be used as a reference and the second arm contains the analyte. Therefore, the optical difference can be realized by scanning and analyzing the arms. The proposed switch can be used to transfer light from the reference arm to the other one. Finally, fabrication of the proposed PCFs is believed to be attainable with a high feasibility and is not beyond the realms of today's available technology.

III. Conclusion

A novel nonlinear switch based on three-core-doped PCF is reported. It is found that the switching operation is sensitive to the irregular structure around the doped core. Our simulations show that a periodic power exchange between the upper and lower cores can be achieved by adjusting the gain. It is also found that independent light propagation in the fiber core can take place for a certain value of the gain. It is shown that the birefringence increases with the increase in the gain. Effective mode area and nonlinear coefficient parameter of the proposed switch have been reported. These properties are important in the context of confinement, bending and splicing losses, along with NA. Finally, dispersion properties of proposed design have been presented. Ultraflattened dispersion is achieved when doped or undoped central cores are used for wavelengths between 1.4 and $1.8\ \mu$m. The proposed nonlinear PCF switch with desired properties as reported here will have a great impact on future applications such as wideband supercontinuum generation, ultrashort soliton pulse transmission, and WDM transmission [18], [21].

References

[1] F. D. Teodoro and P. R. Hoffman, "Tunable, linearly polarized, intrinsically single-mode fiber laser using a 40-μm core-diameter Yb-doped photonic-crystal fiber," *Opt. Commun.*, vol. 252, pp. 111–116, 2005.

[2] N. Y. Joly, F. G. Omenetto, A. Efimov, A. J. Taylor, J. C. Knight, and P. S. J. Russell, "Competition between spectral splitting and Raman frequency shift in negative-dispersion slope photonic crystal fiber," *Opt. Commun.*, vol. 248, pp. 281–285, 2005.

[3] I. D. Chremmos, G. Kakarantzas, and N. K. Uzunoglu, "Modeling of a highly nonlinear chalcogenide dual-core photonic crystal fiber coupler," *Opt. Commun.*, vol. 251, pp. 339–345, 2005.

[4] J. C. Knight, T. A. Birks, P. S. J. Russell, and D. M. Atkin, "All-silica single-mode optical fibre with photonic crystal cladding," *Opt. Lett.*, vol. 21, pp. 1547–1549, 1996.

[5] T. A. Birks, J. C. Knight, B. J. Mangan, and P. S. J. Russell, "Photonic crystal fibres: An endless variety," *IEICE Trans. Electron.*, vol. E84-C, pp. 585–592, 2001.

[6] J. Broeng, D. Mogilevstev, S. E. Barkou, and A. Bjarklev, "Photonic crystal fibres: A new class of optical waveguides," *Opt. Fiber Technol.*, vol. 5, pp. 305–330, 1999.

[7] K. Saitoh and M. Koshiba, "Single-polarization single-mode photonic crystal fibres," *IEEE Photon. Technol. Lett.*, vol. 15, no. 10, pp. 1384–1386, Oct. 2003.

[8] Y. Tsuchida, K. Saitoh, and M. Koshiba, "Design of single-moded holey fibers with large-mode-area and low bending losses: The significance of the ring-core region," *Opt. Exp.*, vol. 15, pp. 1794–1803, 2007.

[9] F. Zhang, P. L. Chu, R. Lai, and G. R. Chen, "Dual-wavelength chaos generation and synchronization in erbium-doped fiber lasers," *IEEE Photon. Technol. Lett.*, vol. 17, no. 3, pp. 549–551, Mar. 2005.

[10] G. C. Valley, "Modeling cladding-pumped Er/Yb fiber amplifiers," *Opt. Fiber Technol.*, vol. 7, pp. 21–44, 2001.

[11] A. Cucinotta, F. Poli, and S. Selleri, "Design of erbium-doped triangular photonic-crystal-fiber-based amplifiers," *IEEE Photon. Technol. Lett.*, vol. 16, no. 9, pp. 2027–2029, Sep. 2004.

[12] A. V. Yulin, D. Skryabin, and P. S. J. Russell, "Four-wave mixing of linear waves and solitons in fibers with higher-order dispersion," *Opt. Lett.*, vol. 29, pp. 2411–2413, 2004.

[13] M. Janos and R. A. Minasian, "Measurement of pump induced refractive index change in erbium-doped optical fiber," *Electron. Lett.*, vol. 33, pp. 78–80, 1997.

[14] S. C. Fleming and S. C. Whitley, "Measurement and analysis of pump-dependent refractive index and dispersion effects in erbium-doped fiber amplifiers," *IEEE J. Quantum Electron.*, vol. 32, no. 7, pp. 1113–1112, Jul. 1996.

[15] Y. Chen, A. W. Snyder, and D. N. Payne, "Twin core nonlinear couplers with gain and loss," *IEEE J. Quantum Electron.*, vol. 28, no. 1, pp. 239–245, Jan. 1992.
[16] S. R. Friberg, M. K. Oliver, M. J. Andrejco, M. A. Safi, and P. W. Smith, "Ultrafast all-optical switching in a dual-core fiber nonlinear coupler," *Appl. Phys. Lett.*, vol. 51, pp. 1135–1137, 1987.
[17] T. Tanabe, M. Notomi, S. Mitsugi, A. Shinya, and E. Kuramochi, "Fast bistable all-optical switch and memory on a silicon photonic crystal on-chip," *Opt. Lett.*, vol. 30, pp. 2575–2577, 2005.
[18] D. S. Moon, U.-C. Paek, and Y. Chung, "Multi-wavelength lasing oscillations in an erbium-doped fiber laser using few-mode fiber Bragg grating," *Opt. Exp.*, vol. 12, pp. 6147–6152, 2004.
[19] Y. O. Barmenkov, A. Ortigosa-Blanch, A. Diez, J. L. Cruz, and M. V. Andrés, "Time-domain fiber laser hydrogen sensor," *Opt. Lett.*, vol. 29, pp. 2461–2463, 2004.
[20] X.-M. Liu, "Four-wave mixing self-stability based on photonic crystal fiber and its applications on erbium-doped fiber lasers," *Opt. Commun.*, vol. 260, pp. 554–559, 2004.
[21] N. G. R. Broderick, T. M. Monro, P. J. Bennet, and D. J. Richardson, "Nonlinearity in holey optical fibers: Measurement and future opportunities," *Opt. Lett.*, vol. 24, pp. 1395–1397, 1999.
[22] K. Saitoh, Y. Sato, and M. Koshiba, "Coupling characteristics of dual-core photonic crystal fiber couplers," *Opt. Exp.*, vol. 11, pp. 3188–3195, 2003.
[23] K. Thyagarajan and S. Pilevar, "Resonant tunneling three-waveguide polarization splitter," *J. Lightw. Technol.*, vol. 10, no. 10, pp. 1334–1337, Oct. 1992.
[24] L. Zhang, C. Yang, C. Yu, T. Luo, and A. E. Willner, "PCF-based polarization splitters with simplified structures," *J. Lightw. Technol.*, vol. 23, no. 11, pp. 3558–3565, Nov. 2005.
[25] L. Zhang and C. Yang, "Polarization splitter based on photonic crystal fibers," *Opt. Exp.*, vol. 11, pp. 1015–1020, 2003.
[26] B. J. Mangan, J. C. Knight, T. A. Birks, P. S. J. Russell, and A. H. Greenaway, "Experimental study of dual-core photonic crystal fibre," *Electron. Lett.*, vol. 36, pp. 1358–1359, 2000.
[27] A. E. Siegman, "Propagating modes in gain-guided optical fibers," *J. Opt. Soc. Amer. A*, vol. 20, pp. 1617–1628, 2003.
[28] J. Ju, W. Jin, and M. S. Demokan, "Two-mode operation in highly birefringent PCF," *IEEE Photon. Technol. Lett.*, vol. 16, no. 11, pp. 2472–2474, Nov. 2004.
[29] H. Ademgil and S. Haxha, "Highly birefringent photonic crystal fibres with ultra-low chromatic dispersion and low confinement losses," *J. Lightw. Technol.*, vol. 26, no. 4, pp. 441–448, Feb. 2008.
[30] S. Haxha and H. Ademgil, "Novel design of photonic crystal fibres with low confinement losses, nearly zero ultra-flatted chromatic dispersion, negative chromatic dispersion and improved effective mode area," *Opt. Commun.*, vol. 281, pp. 278–286, 2008.
[31] T. Gorman and S. Haxha, "Optimisation of Z-cut lithium niobate electrooptic modulator with profiled metal electrodes and waveguides," *J. Lightw. Technology*, vol. 25, no. 12, pp. 3722–3729, Dec. 2007.
[32] F. AbdelMalek, W. Belhadj, S. Haxha, and H. Bouchriha, "Realization of a high coupling efficiency by employing a concave lens based on two-dimensional photonic crystals with a negative refractive," *J. Lightw. Technol.*, vol. 25, no. 10, pp. 3168–3174, Oct. 2007.
[33] K. Saitoh and M. Koshiba, "Full-vectorial imaginary-distance beam propagation method based on a finite element scheme: Application to photonic crystal fibres," *IEEE J. Quantum Electron.*, vol. 38, no. 7, pp. 927–933, Jul. 2002.
[34] S. Guo, F. Wu, S. Albin, H. Tai, and R. Rogowski, "Loss and dispersion analysis of micro-structured fibres by finite-difference method," *Opt. Exp.*, vol. 12, pp. 3341–3352, 2004.
[35] P. L. Chu and B. Wu, "Optical switching in twin-core erbium-doped fibers," *Opt. Lett.*, vol. 17, pp. 255–257, 1992.
[36] R. A. Betts, T. Tjugiarto, Y. L. Xue, and P. L. Chu, "Nonlinear refractive index in erbium doped optical fiber: Theory and experiment," *IEEE J. Quantum Electron.*, vol. 27, no. 4, pp. 908–913, Apr. 1991.
[37] J. Ju, W. Jin, and M. S. Demokan, "Properties of a highly birefringent photonic crystal fiber," *IEEE Photon. Technol. Lett.*, vol. 15, no. 10, pp. 1375–1377, Oct. 2003.
[38] A. Ortigosa-Blanch, J. C. Knight, W. J. Wadsworth, J. Arriaga, B. J. Mangan, T. A. Birks, and P. S. J. Russell, "Highly birefringent photonic crystal fibers," *Opt. Lett.*, vol. 25, pp. 1325–1327, 2000.
[39] I. K. Hwang, Y. J. Lee, and Y. H. Lee, "Birefringence induced by irregular structure in photonic crystal fiber," *Opt. Exp.*, vol. 11, pp. 2799–2806, 2003.
[40] K. Reichenbach and C. Xu, "The effects of randomly occurring nonuniformities on propagation in photonic crystal fibers," *Opt. Exp.*, vol. 13, pp. 2799–2807, 2005.
[41] F. Poletti, V. Finazzi, T. M. Monro, N. G. R. Broderick, V. Tse, and D. J. Richardson, "Inverse design and fabrication tolerances of ultra-flattened dispersion holey fibers," *Opt. Exp.*, vol. 13, pp. 3728–3736, 2005.
[42] N. A. Mortensen, "Effective area of photonic crystal fibers," *Opt. Exp.*, vol. 10, pp. 341–348, 2002.
[43] A. Huttunen and P. Törmä, "Effect of wavelength dependence of nonlinearity, gain, and dispersion in photonic crystal fiber amplifiers," *Opt. Exp.*, vol. 13, pp. 4286–4295, 2005.
[44] D. Ferrarini, L. Vincetti, M. Zoboli, A. Cucinotta, and S. Selleri, "Leakage properties of photonic crystal fibres," *Opt. Exp.*, vol. 10, pp. 1314–1319, 2002.
[45] F. Zolla, G. Renversez, A. Nicolet, B. Kuhlmey, S. Guenneau, and D. Felbacq, *Foundations of Photonic Crystal Fibres*. London, U.K.: Imperial Collage Press, 2005.
[46] W. H. Reeves, J. C. Knight, P. S. J. Russell, and P. J. Roberts, "Demonstration of ultra-flattened dispersion in photonic crystal fibers," *Opt. Exp.*, vol. 10, pp. 609–613, 2002.
[47] S. Yang, Y. Zhang, X. Peng, Y. Lu, S. Xie, J. Li, W. Chen, Z. Jiang, J. Peng, and H. Li, "Theoretical study and experimental fabrication of high negative dispersion photonic crystal fiber with large area mode field," *Opt. Exp.*, vol. 14, pp. 3015–3023, 2006.

Fathi AbdelMalek received the Ph.D. degree from the Ecole Centrale de Lyon, Lyon, France, in 1999.

He was a Research Associate and a Research Fellow at various U.S. and U.K. universities, where he carried out research on sensors, grating for telecommunication and photonics. He is currently an Associate Professor in the Department of Physics and Engineering, National Institute of Applied Sciences and Technology (INSAT), Tunis, Tunisia. He is also with the College of Optical Sciences, University of Arizona, Tucson, AZ. His current research interests include nanophotonics, nanoplasmonic crystals, metamaterials, microstructured fibers, developing novel approaches to subcellular imaging, quantum dots, biosensors, and numerical techniques such finite-difference time domain (FDTD) and finite-element (FE) methods. He is engaged in the design of integrated nanophotonic devices.

Hongbo Li received the M.S. degree in optical sciences and the Ph.D. degree from the University of Arizona, Tucson.

He is currently with Aither Engineering, Lanham, MD, where he is engaged in laser induced breakdown spectroscopy (LIBS) systems and fiber-optic sensors. He is also with the College of Optical Sciences, University of Arizona. He was engaged in research on developing novel compact high-power fiber lasers and vertical-external-cavity surface-emitting lasers.

Axel Schülzgen received the Ph.D. degree in physics from Humboldt-University Berlin, Berlin, Germany, in 1992.

He is currently an Associate Research Professor at the College of Optical Sciences, University of Arizona, Tucson. His current research interests include development of fiber lasers, the investigation of advanced materials, novel nonlinear optical effects, ultrafast nonlinear optics, and coherent effects in light–matter interaction.

Jerome V. Moloney received the B.Sc. degree from the University College, Cork, Ireland, in 1970, and the Ph.D. degree from the University of Western Ontario, London, ON, Canada, in 1977.

He is currently a Professor of mathematics, a Professor of optical sciences, and a Visiting Professor of computational physics at the University College Cork. Since 1985, he has been a Professor in the Department of Mathematics and Optical Sciences Center, University of Arizona, Tucson, where he is the Director of the Arizona Center for Mathematical Sciences, and has been with the Optical Sciences Center since 1979, in several capacities: Research Associate Professor (1984–1985), Research Assistant Professor (1981–1984), and Research Associate (1979–1981). He was a Reader in physics (1984–1990) at Heriot-Watt University, Edinburgh, U.K., and a Research Associate (1977–1979) at the Universitate Bielefeld, Germany. His current research interests include mathematical modeling and simulation of photonics systems including semiconductor lasers, fiber lasers, and photonic Bragg and photonic crystal fibers, fundamental theory of semiconductor lasers including microscopic physics, modeling high-power femtosecond atmospheric light strings, nonlinear theory of partial differential equations and chaos synchronizations in extended complex spatiotemporal interacting systems, and sophisticated algorithm development for large-scale computational photonics systems simulations including adaptive mesh refinement and parallelization distributed and shared memory supercomputer platforms.

Prof. Moloney is associated with the National Research Council, the Naval Studies Board, and the Workshop on Mathematics. He is a member of the Mathematics in Material Sciences at the Society for Industrial and Applied Mathematics. He is a member of the organizing committee at the Institute of Mathematics and Its Applications, University of Minnesota, and an organizer of the Workshop on Nonlinear Optical Materials.

Nasser Peyghambarian (A'04–M'04) received the B.S. degree from Pahlavi University, Shiraz, Iran, in 1976 and the M.S. degree and the Ph.D. degree in solid-state physics from Indiana University, Bloomington, in 1979 and 1982, respectively. His doctoral work specialized in optical properties of semiconductors.

He is currently a Professor of optical sciences with the College of Optical Sciences and Engineering, University of Arizona, Tucson. His current research interests include optical telecommunication, fiber optics, fiber amplifiers and fiber lasers, lasers, femtosecond laser spectroscopy and dynamics of optical phenomena in semiconductors and organic materials, nonlinear photonics and high-speed optical switching, polymer optoelectronics, and organic light-emitting diodes and lasers.

Prof. Peyghambarian is a Fellow of the American Physical Society, the Optical Society of America, and the International Society for Optical Engineers (SPIE).

Huseyin Ademgil received the B.Sc. degree in electronic engineering in 2005 from the Eastern Mediterranean University, Famagusta, Cyprus, and the M.Sc. degree in broadband and mobile communication networks in 2006 from the University of Kent, Canterbury, U.K., where he is currently working toward the Ph.D. degree in photonics.

His current research interests include finite-element modeling of photonic devices.

Shyqyri Haxha (S'01–M'04–SM'06) received the M.Sc. and Ph.D. degrees from the City University London, London, U.K., in 2000 and 2004, respectively.

In February 2004, he joined the Broadband and Wireless Communications Group, Electronics Department, Kent University, Canterbury, U.K., as a Lecturer. His current research interests include photonic crystal devices, metamaterials, photonic crystal fibers, surface plasmon polaritons, high-speed modulators, and optical code division multiple access (OCDMA) systems.

Dr. Haxha is a member of the Optical Society of America (OSA) and the Institution of Engineering and Technology (IET), London, U.K. In April 2003, he was awarded the SIM Postgraduate Award from the Worshipful Company of Scientific Instrument Makers in Cambridge, U.K., for his highly successful contribution in research.